p120 catenin is required for morphogenetic movements involved in the formation of the eyes and the craniofacial skeleton in *Xenopus*

Malgorzata Ciesiolka[1,*], Mieke Delvaeye[1,*], Griet Van Imschoot[1], Veerle Verschuere[1], Pierre McCrea[3], Frans van Roy[2] and Kris Vleminckx[1,‡]

[1]Developmental Biology Unit and [2]Molecular Cell Biology Unit, Department of Molecular Biomedical Research, Flanders Interuniversity Institute for Biotechnology (VIB) – Ghent University, Technologiepark 927, B-9052 Ghent, Belgium
[3]Department of Biochemistry and Molecular Biology, Program in Genes and Development, University of Texas, M. D. Anderson Cancer Center, 1515 Holcombe Boulevard, Houston, TX 77030, USA

*Authors contributed equally
‡Author for correspondence (e-mail: kris.vleminckx@dmbr.ugent.be)

Accepted 28 April 2004
Journal of Cell Science 117, 4325-4339 Published by The Company of Biologists 2004
doi:10.1242/jcs.01298

Summary

During *Xenopus* development, p120 transcripts are enriched in highly morphogenetic tissues. We addressed the developmental function of p120 by knockdown experiments and by expressing E-cadherin mutants unable to bind p120. This resulted in defective eye formation and provoked malformations in the craniofacial cartilage structures, derivatives of the cranial neural crest cells. Closer inspection showed that p120 depletion impaired evagination of the optic vesicles and migration of cranial neural crest cells from the neural tube into the branchial arches. These morphogenetic processes were also affected by p120-uncoupled cadherins or E-cadherin containing a deletion of the juxtamembrane domain. Irrespective of the manipulation that caused the malformations, coexpression of dominant-negative forms of either Rac1 or LIM kinase rescued the phenotypes. Wild-type RhoA and constitutively active Rho kinase caused partial rescue. Our results indicate that, in contrast to invertebrates, p120 is an essential factor for vertebrate development and an adequate balance between cadherin activity and cytoskeletal condition is critical for correct morphogenetic movements.

Supplemental data available online

Key words: Embryogenesis, Cadherins, Catenins, Rho GTPases, Xenopus

Introduction

Cadherins comprise a superfamily of cell-cell adhesion molecules that are involved in intercellular adhesion in a wide variety of cell types. Modulation of the strength of cell-cell adhesion is essential during morphogenetic processes involving cell movements and tissue rearrangements. Functional inactivation of cadherins during these events seems to be an important step in the regulation of the balance between cell adhesion and motility (Gumbiner, 2000; Perez-Moreno et al., 2003; Tepass et al., 2000). Dysfunction of this balance is often observed in cancer cells, where the loss of E-cadherin expression and disruption of cell-cell adhesion correlates with tumor invasion (Mareel and Leroy, 2003). While physical interaction between two cadherins is a prerequisite for intercellular adhesion, it is clearly not of sufficient force. Adhesive strength is considerably enhanced by clustering of the adhesion molecules in the membrane, and by their physical interaction with the cytoskeleton (Gumbiner, 2000). Interestingly, cadherins are also capable of signaling to the cytoplasm (Yap and Kovacs, 2003; Braga, 2002). These signals can change the behavior of the cell and the organization of the cytoskeleton. Hence, one can envision a scenario in which the homophilic interaction between cadherins on neighboring cells not only provides physical adhesion, but also locks the cells in an immobile condition via signaling.

Cadherins are associated in the cytoplasm with catenins, which link them to the cytoskeleton and can regulate their adhesive functions. The highly conserved distal region of the cytoplasmic tail of cadherin binds β-catenin or plakoglobin (γ-catenin). These proteins can interact with α-catenin, which provides a direct or indirect link with the actin cytoskeleton, a link that is required for development of strong adhesion. The second highly conserved region of the cadherin cytoplasmic tail is localized near the membrane, and binds several p120 catenin family members, including p120 catenin (p120), ARVCF and δ-catenin/NPRAP. This domain was also identified as a binding site for the ubiquitin-ligase Hakai and presenilin 1, both of which may be involved in the trafficking/recycling of cadherins (Fujita et al., 2002; Uemura et al., 2003; Marambaud et al., 2002; Baki et al., 2001). Functional analysis of the cytoplasmic domain of E- and N-cadherin identified the juxtamembrane domain (JMD) as a domain interfering with cell motility/invasion, neuronal outgrowth and ectodermal cell adhesion (Chen, 1997; Kintner, 1992; Riehl, 1996). Other studies implicated the JMD in positive and/or negative regulation of cell adhesion (reviewed

by Anastasiadis and Reynolds, 2000). Emerging evidence suggests that p120 is a potential regulator of the adhesive strength of cadherins. Whereas some studies demonstrated a positive role for p120 in the dimerization and clustering of cadherins in the plasma membrane and in cell-cell junction formation, others indicated that p120 has a negative effect on cadherin-mediated cell-cell adhesion. In an effort to unify these conflicting data, a model has been proposed in which post-translational modifications of p120, probably including phosphorylations, lead to its 'activation' or 'inactivation' (Anastasiadis and Reynolds, 2000). In this model, p120 acts as a switch that can promote either strong or weak adhesion. Surprisingly, experiments in *Drosophila* have indicated that a p120-uncoupled DE-cadherin mutant can act as a perfect substitute for wild-type DE-cadherin, making it unlikely in this system that the binding of p120 is important for the functional regulation of DE-cadherin (Pacquelet et al., 2003). Very recent experiments on mammalian cell lines demonstrated that p120, in addition to influencing cadherin function directly, influences the stabilization and recycling of cadherin/catenin complexes at the plasma membrane (Chen et al., 2003; Davis et al., 2003; Xiao et al., 2003). Moreover, it has been found that p120 binds to kinesin and microtubules and hence may assist in targeting of cadherin/catenin complexes to sites of cell-cell contact (Chen et al., 2003; Franz and Ridley, 2003).

p120 has been shown to modulate the activity of Rho GTPases, leading to morphological changes and increased cell migration (Anastasiadis et al., 2000; Grosheva et al., 2001; Noren et al., 2000). The Rho GTPases represent a highly conserved family of molecules that regulate a variety of cellular functions, including the dynamics of the actin cytoskeleton, cell adhesion, transcription, cell growth and membrane trafficking (reviewed by Etienne-Manneville and Hall, 2002). The mechanism by which p120 regulates the Rho GTPases is still not well understood, but it has been proposed that it involves direct interaction of p120 with RhoA or Vav2, which is a guanine nucleotide exchange factor (GEF) for Rac1, Cdc42 and RhoA (Anastasiadis et al., 2000; Grosheva et al., 2001; Noren et al., 2000). The ability of Rho family members to regulate the adhesive and motile behavior of cells makes them good candidates for involvement in morphogenetic processes during embryonic development, where precise shape changes, tissue rearrangements and cell movements are required. Substantial information regarding the function of Rho GTPases has been derived from studies in *Drosophila*, but recent evidence suggests that Rho proteins are important for morphogenesis in vertebrates as well (Van Aelst and Symons, 2002).

The function of p120 during development has recently been addressed in *Drosophila*. Null alleles for p120 look phenotypically normal, but when analyzed in crosses, the p120 deficiency enhances the phenotypes of DE-cadherin and Armadillo mutants (Myster et al., 2003). Comparable results were obtained for the *Caenorhabditis elegans* ortholog of p120, JAC-1 (Pettitt et al., 2003). Furthermore, it has been reported that Rho1, the *Drosophila* ortholog of RhoA, interacts physically and functionally with p120 (Magie et al., 2002). The role of p120 in vertebrate development was analyzed by overexpression and recently also by morpholino-mediated depletion in *Xenopus* embryos (Geis et al., 1998; Paulson et al., 1999; Fang et al., 2004). While overexpression of p120 in the dorsal mesoderm induced severe gastrulation defects, the depletion of p120 in addition affected convergent extension movements. Interestingly, in agreement with reports in cell culture, the effects of p120 depletion could be rescued by co-injection of dominant negative RhoA and dominant active Rac (Fang et al., 2004).

In this study we wanted to explore the role of p120 in vertebrate development. We report the cloning of the *Xenopus* p120 ortholog and analysis of the expression pattern in the early embryo. We found that p120 transcripts are highly enriched in the eye vesicles and in the branchial arches. Consequently, we investigated the morphogenetic repercussions induced in *Xenopus* embryos by depletion of p120, and by expression of point and deletion mutants of E-cadherin that are unable to bind p120. We targeted our injections to a region contributing mainly to the (neuro)ectodermal tissues of the future head region so that we would not interfere with gastrulation and convergent extension movements. Depletion of p120 and overexpression of the E-cadherin mutants induced perturbations in the developing eyes and in the craniofacial cartilage skeleton, a derivative of the cranial neural crest. We also demonstrate that dominant negative forms of Rac and LIM kinase, and to a lesser extent wild-type RhoA and constitutively active Rho kinase, rescue the phenotypes induced by p120 depletion or ectopic mutant cadherins. Our results indicate that p120 is crucially involved in regulating morphogenetic cell movements in the anterior region of early embryo, most likely by modifying the activity of the cadherins at the membrane, and coordinating their functional interactions with the cytoskeleton.

Materials and Methods

Reverse transcription and PCR

Total RNA was extracted from XTC cells, *Xenopus* adult tissues and embryos from stage 0 to stage 39 using RNAzol (Wak-Chemie Medical, GMBH) according to the manufacturer's instructions. To detect Xp120 transcripts, cDNA was generated from 1 μg of total RNA using Superscript reverse transcriptase (Life Technologies) as described previously (Keirsebilck et al., 1998). cDNA (3 μl) was amplified using Taq polymerase (Boehringer Mannheim) or Pfu polymerase and the primers 5′ TAGGAGGCCTGGAGTGTGA 3′ and 5′ ATCAGTGGCATTGTTGAATC 3′.

Plasmid constructs

To generate plasmids for RNA injection, the cDNAs encoding the Xp120 isoforms were amplified from stage 30 *Xenopus* embryos using Pfu DNA polymerase, with primers incorporating *Eco*RI (5′ end) and *Spe*I (3′ end) restriction sites. Amplified fragments were sequenced and cloned in the *Eco*RI-*Xba*I sites of pCS2+ (Turner and Weintraub, 1994). The full-length mouse E-cadherin (mE-cad) cDNA was isolated from the pBATEM2 plasmid by digestion with *Bgl*II and *Xba*I and subcloned in the *Bam*HI and *Xba*I sites of the pCS2+ vector. The mE-cad cDNA sequence in between *Xho*I and *Nhe*I (998 bp) was replaced by a fragment derived from the pSUMΔC8 plasmid (Ozawa et al., 1990). The resulting pCS2+mEcadhΔJMD construct contains a deletion of 31 AA in the JMD of the mE-cad cDNA.

The plasmid pSp64T-XEcad, carrying the full-length *Xenopus* E-cadherin (XE-cad) cDNA, was digested with *Cla*I and *Xba*I, and the fragment corresponding to the full length XE-cad cDNA was cloned into the corresponding sites of the pCS2+ vector. The pCS2+XEcad

plasmid was used in site directed mutagenesis (Stratagene) to generate the p120-uncoupled XE-cadh750AAA and the XE-cadh753AAA mutants. For in vitro transcription, the full length human WT-RhoA, CA-RhoA^{V14}, DN-RhoA^{N19}, CA-Rac1^{V12} and DN-Rac1^{V12N17} were subcloned from the pcDNA3.1 vector into the pCS2+ plasmid, and CA-ROCK was subcloned from pEF-bos-myc into the pCS2+plasmid.

RNA and morpholino injections

For RNA injections, all constructs were linearized with *Not*I, except for WT/XLK1 and WT/XLK1(KD) (encoding WT and DN LIMK), which were linearized with E*co*RI. Capped mRNAs were synthesized in vitro from linearized plasmids using SP6 polymerase (Promega). Integrity of RNA was checked on denaturating agarose gels. The morpholinos used were p120 MO 5′ ACTCTGGCTCATCC-ATATAGAAAGG 3′ and a standard control oligo as negative control (Gene Tools).

Xenopus eggs were fertilized by standard methods (Newport and Kirschner, 1982), dejellied with 2% cysteine (pH 8.0), rinsed and incubated in 0.1× MMR (10 mM NaCl, 0.2 mM KCl, 0.1 mM $MgSO_4$, 0.2 mM $CaCl_2$, 0.5 mM Hepes, pH 7.4). Embryos were placed in 1× MMR containing 6% Ficoll, and injected with mRNA. Two hours after injection, embryos were transferred to 0.1× MMR and cultured at 17°C until they had reached the neurula stage. Stages of embryonic development were determined according to a published table of *Xenopus laevis* development (Nieuwkoop and Faber, 1994).

Cell tracing in embryos

For the tracing experiments with Rhodamine, embryos were injected in 1 cell at the 32-cell stage with dextran, tetramethylRhodamine (M_r 70×10^3), lysine fixable (Molecular Probes) in combination with morpholino or RNA. Embryos were monitored with a Leica MZFLIII fluorescence stereomicroscope, and pictures were taken with a Leica DC 300F camera. Desired stages were fixed for 1 hour in MEMFA at room temperature, embryos were washed 3 times in PBS and soaked overnight in 20% sucrose/PBS. Embryos were embedded in cryo-embedding compound (Microm) and sections of 12 μm were cut. Sections were dried at room temperature and mounted with Vectashield containing DAPI (VECTOR laboratories). Images were obtained with an Axiophot microscope (Carl Zeiss) using a 10× objective equipped with a digital camera (MicroMAX, RS Photometrics), and processed using Metamorph Image software (Universal Imaging).

Migration of the NCCs was examined by injecting dextran, DMNB-caged Fluorescein, M_r 10×10^3, anionic (Molecular Probes) in combination with morpholino or RNA in the dorsal-animal region, which gives rise to the cranial neural crest. Embryos were irradiated at stage 14 with the UV light of an Axiophot microscope (Carl Zeiss) using the 10× objective to activate the caged Fluorescein. Embryos were monitored with a Leica MZFLIII fluorescence stereomicroscope.

Whole-mount in situ hybridization and Alcian Blue staining

A plasmid containing full-length Xp120iso1 cDNA was linearized with *Nde*I or *Sna*BI and used to prepare sense and antisense riboprobes, which were digoxigenin-labeled according to the manufacturer's instructions (Boehringer Mannheim). Whole-mount in situ hybridization and sectioning of stained specimens were performed as described (Bellefroid et al., 1996). Embryos were bleached for 1-2 hours under UV in Mayor bleaching solution (1% H_2O_2, 5% formamide, 0.5× SSC) and incubated in 2:1 (v/v) benzyl benzoate/benzyl alcohol clearing solution for inspection with a stereomicroscope (Carl Zeiss). For histological analysis, embryos were fixed in MEMFA at room temperature for 1 hour, rinsed twice in 70% PBS for 10 minutes, dehydrated in a series of 10 minute washes in ethanol/PBS, and transferred to JB-4 embedding medium (Polysciences). Sections of 5 μm were made with a Universal Heavy Duty Microtome and stained with Hematoxilin and Eosin. Alcian Blue staining was performed as described (Pasqualetti et al., 2000).

Immunoblotting

For western blot detection, injected embryos were collected at different time points, lysed in NP-40 lysis buffer (0.5% NP-40, 150 mM NaCl, 50 mM Tris pH 7.5, 2 mM EDTA, 0.02% NaN_3) and cleared by centrifugation for 5 minutes at 4°C. Laemmli sample buffer was added to the supernatants and the equivalent of three embryos was loaded per lane and separated in an 8% SDS-polyacrylamide gel. The proteins were blotted onto a nitrocellulose membrane and detected with polyclonal anti-Xp120, anti-C-cadherin, mouse monoclonal anti-E-cadherin, mouse monoclonal anti-Myc tag 9E12, rat monoclonal anti-N-cadherin (Zymed), and rat monoclonal anti-mE-cadherin ECCD-2 (Sigma). After washing, blots were incubated with HRP-conjugated anti-rabbit, anti-mouse and anti-rat IgGs, respectively (Amersham Pharmacia Biotech), followed by washing and developing with enhanced chemiluminescence (ECL, Amersham Pharmacia Biotech).

Immunofluorescence and confocal microscopy

For immunohistological staining of sections, embryos were fixed in DMSO/methanol overnight at –20°C, rinsed in PBS and soaked for 24 hours in 15% gelatin/15% sucrose. Afterwards embryos were embedded in cryo-embedding compound (Microm). Sections of 12 μM were cut. Sections were dried for 1 hour at room temperature, dipped for 2 minutes in acetone, rehydrated in PBS, washed for 20 minutes in PBS/Tween and incubated with the primary antibody (Decma-1, Sigma, 1:1000) overnight at 4°C. After incubation with the primary antibody, sections were washed 3 times with PBS/Tween and incubated with the secondary antibody (anti-rat Alexa 488, 1:500) for 2 hours at 30°C. Afterwards sections were washed 3 times with PBS/Tween and incubated in DAPI/PBS for 15 minutes. Sections were washed again 2 times with PBS and incubated in PBS containing 0.1% Eriochrome Black for 5-15 minutes (Sigma) to mask autofluorescence. Sections were mounted with vectashield (VECTOR laboratories). Images were obtained with an Axiophot microscope (Carl Zeiss) using a 20× objective; the microscope was equipped with a digital camera (MicroMAX, RS Photometrics) and Metamorph Image software (Universal Imaging). The sections were also examined with an inverted confocal Laser Scan Microscope 410 (Carl Zeiss) using an Argon laser (488 nm) and appropriate settings. The confocal images in Fig. 10B were selected from the 19 images made by z-sectioning (1 μm Z-spacing) on living embryos.

Results

Isolation of the *Xenopus* p120 ortholog

We isolated sequences encoding the *Xenopus* p120 ortholog in a yeast two-hybrid screening, using the cytoplasmic tail of *Xenopus* N-cadherin lacking the β-catenin binding site as bait. The merged cDNA sequences indicated two open reading frames of 2577 and 2355 bp. Alignment of the deduced amino acid sequence of the longer open reading frame with the human p120 isoform 1ABC revealed 48% identity and 62% similarity (Fig. 1A). Sequence alignment with other p120 family members indicates that the isolated clones indeed represent the *Xenopus* p120 ortholog (Table 1). Particularly high sequence conservation was observed in the armadillo domain and within the N-terminal coiled-coil region, with less sequence homology present at the C- and remaining N-terminal regions. Sequence

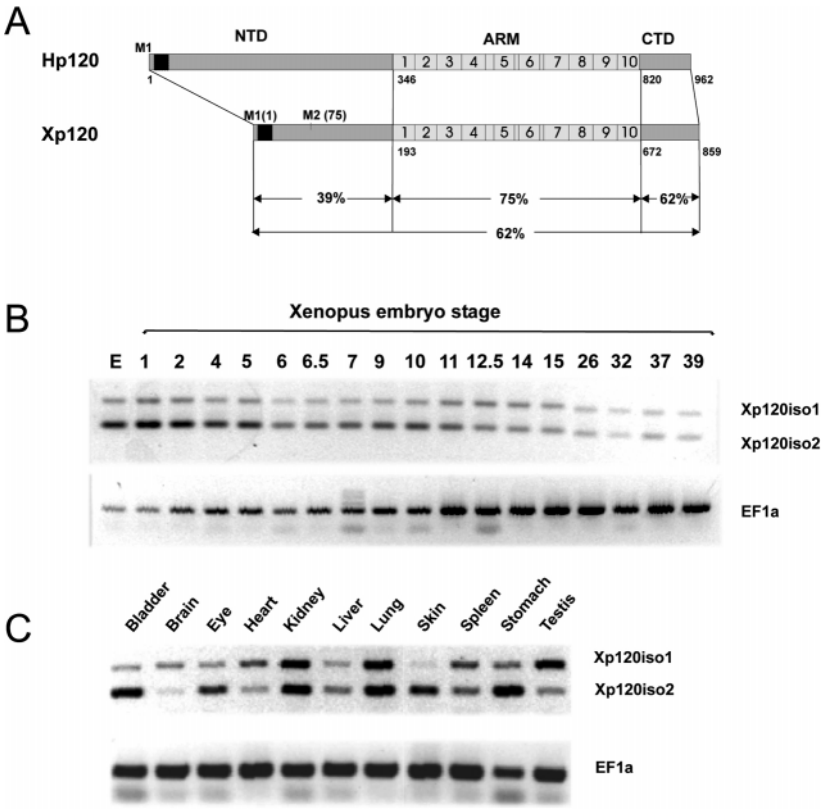

Fig. 1. Comparison of *Xenopus* and human p120 sequences and RT-PCR analysis of p120 expression during early embryonic development and in adult *Xenopus* tissues. (A) Linear representation of the amino acid sequence similarities between hp120 1ABC and Xp120 isoform 1. In the *Xenopus* p120 sequence, two translational start sites (M1 at position 1 and M2 at position 75) are indicated. Isoform 2 is derived by splicing, which takes place upstream of M1. A conserved coiled-coil domain in the N-terminal region of p120 is shown (black box). Percentages indicate the similarities of the sequences of Xp120 isoform 1 and hp120 1ABC for the whole protein (calculated with Needleman-Wunsch algorithm from EMBOSS) and for the N-terminal domain (NTD), the central domain (ARM) or the C-terminal domain (CTD) (calculated with the Clustal W method from the GCG program, BEN, Brussels). The *Xenopus* p120 sequence data are available from EMBL/GenBank under accession numbers AF150743 and AF150744. (B) A semi-quantitative RT-PCR evaluation of Xp120 isoform expression in embryos at different developmental stages and (C) in selected tissues derived from an adult frog. The PCR band of 500 bp is amplified when the NH_2-terminal insert of 210 nucleotides is present (Xp120iso1). The band of 290 bp represents the shorter isoform of Xp120 (Xp120iso2). An RT-PCR reaction of elongation factor 1 (EF1a) was used as a loading control.

analysis showed an alternatively spliced region of 210 nucleotides within the N-terminal region of Xp120, which removes sequences containing an upstream translational start site and directs the use of the second downstream translational start site. Using RT-PCR we confirmed that both p120 transcripts that were identified in the yeast two-hybrid screen are indeed present in *Xenopus* embryos (Fig. 1B) as well as in the XTC cell line (data not shown). In the adult frog, both p120 transcripts were detected in all tissues examined (Fig. 1C). Although up to 48 splicing isoforms are predicted for human p120 (Aho et al., 1999; Keirsebilck et al., 1998), we were unable to detect any additional splicing events for *Xenopus* p120 (data not shown). Moreover, using a mixture of antibodies directed against the N- and C-termini of Xp120 on immunoblot, we detected only a single specific band corresponding to the predicted size of isoform 1 (see section on cadherin levels).

p120 mRNA is enriched in highly morphogenetic regions during *Xenopus laevis* development

To gain insight into the role of p120 during *Xenopus* development, we examined its spatio-temporal expression pattern by semi-quantitative RT-PCR and whole-mount in situ hybridization. Our results demonstrate that p120 is expressed both maternally and during all stages of early embryogenesis. Before gastrulation, the p120 transcript representing the shorter isoform appears to be more abundant (Fig. 1B). In early gastrula stage embryos, p120 is enriched in the animal hemisphere (Fig. 2a). In the late neurula, expression of p120 was enhanced in the anterior region, especially in the optic vesicles (Fig. 2b). At the tailbud stage, inspection of whole embryos (Fig. 2c) or transverse sections (Fig. 2d) indicated that p120 expression was clearly enriched in the head region, particularly in the optic vesicle, ear vesicle, olfactory placode and branchial arches. Weakly elevated expression of p120 was also detected in the somites, the notochord and the pronephros. In summary, while p120 is ubiquitously expressed during development, its levels are particularly high in tissues participating in prominent morphogenetic movements.

Depletion of p120 affects the eyes and the craniofacial skeleton

It was recently reported that depletion of p120 in whole *Xenopus* embryos results in severe gastrulation defects and interferes with convergent extension movements (Fang et al., 2004). Our in situ hybridization data, showing increased expression of p120 mRNA in certain tissues of the anterior

Table 1. Percentages of Xp120 protein identity/similarity with p120 family members

	Hp120	Mp120	Dp120	hARVCF	xARVCF	Hp0071	Hδ-catenin
Xp120	48/62	48/61	28/41	40/54	38/54	26/37	40/52

Full-length protein alignment and calculations of protein identities/similarities were performed using Needleman-Wunsch algorithm as implemented in the needle program from EMBOSS (The European Molecular Biology Open Software Suite).

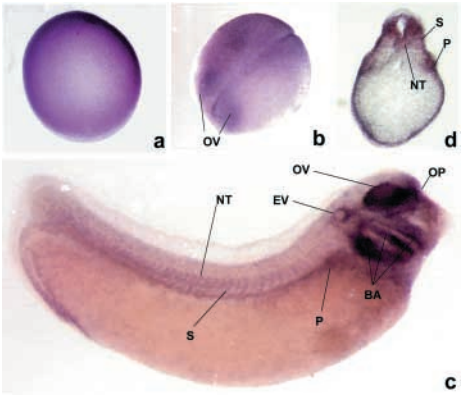

Fig. 2. Analysis of p120 expression in early *Xenopus* embryos by whole mount in situ hybridization. Spatial expression of p120 was evaluated by whole mount in situ hybridization using an antisense Xp120iso1 RNA probe. Expression of p120 is enriched in the animal hemisphere at the blastula stage (a); the optic vesicles (OV) at the neurula stage (b); the optic vesicle (OV), ear vesicle (EV), olfactory placode (OP) and branchial arches (BA) in the head region and also the somites (S), notochord (NT) and pronephros (P) at tailbud (stage 30) (c). (d) Transverse section through a stage 30 tailbud embryo showing increased p120 expression in somites, notochord and pronephros.

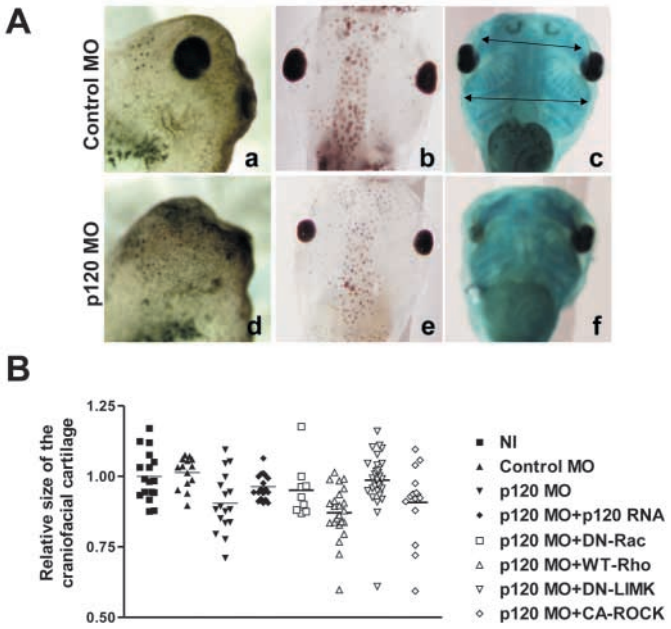

Fig. 3. Expression of p120 morpholino (MO) affects the size of the eyes and cartilage. (A) Injection of p120 MO at 8- to 16-cell stage in the region that gives rise to the head results in the formation of smaller eyes or their complete loss (d,e) compared with control MO-injected embryos (a,b). Tadpoles are shown alive at stages 33 (a,d) and 42 (b,e), or fixed and stained by Alcian Blue to reveal the cartilage structures at stage 46 (c,f). Next to smaller or absent eyes, embryos injected with p120 MO also show smaller craniofacial cartilage structures (f) compared with control MO-injected embryos (c). (B) Graph representing the effect of p120 MO on the size of the craniofacial skeleton. For clarity of the figure, representative experiments are shown. The width of the head was calculated by taking the sum of both arrows indicated in A,c. Values were divided by the average value of non-injected embryos. The head size of embryos injected with p120 MO is statistically different from that of the control population (P=0.0068, Student's t-test). This effect can be rescued by co-injection of RNA encoding Xp120 (30 pg), dominant negative (DN) Rac (33 pg), or DN LIMK (500 pg). Wild type (WT) Rho (125 pg) and CA ROCK (150 pg) are unable to rescue the effect of p120 MO on the size of the head.

region of the embryo, prompted us to determine whether p120 depletion can also interfere with the development of anterior (neuro)ectodermal structures. For this, we injected a morpholino (p120 MO) targeted to the start codon and the 5′ UTR of p120 into the animal region of the two dorsal blastomeres of a 16-cell stage embryo. As a control, we injected a morpholino targeted to an irrelevant sequence (control MO). Dorsal-animal injection targets the region that contributes mainly to head ectodermal structures, such as the cranial neural crest, the retina, the lens, the olfactory placode and the brain (Moody, 1987). When embryos injected with p120 MO were scored at the tailbud or tadpole stages, we observed that eye formation was clearly affected (Fig. 3A, Table 2). In the majority of these embryos, the size of one or both eyes was reduced, or eyes were totally absent. Other anterior structures, such as the prosencephalon and the olfactory placodes and bulbs, were morphologically normal. No phenotype was observed upon injection of up to 50 pg of control MO, and the p120 MO-induced eye phenotype could be rescued by co-injection of Xp120 mRNA (Table 2). Importantly, because our injections were targeted to the dorsal-animal region, the observed eye phenotype does not result from interference of p120 depletion with the activity of the Spemann Organizer and the anterior endomesoderm, two regions involved in patterning of the dorso-anterior axis. The injected region also does not participate in the convergent extension movements of the dorsal mesoderm or the neural ectoderm. Consequently, all injected embryos underwent normal gastrulation and axis elongation.

Interestingly, when p120 MO-injected embryos were grown until stage 45-46, we observed additional developmental abnormalities characterized by smaller craniofacial cartilage structures resulting in reduced width of the head (Fig. 3A and 3B). Staining of the cartilage with Alcian Blue showed that, despite the reduced size, there were no gross morphological abnormalities in the structures of those cartilages (see section on cadherin deletion mutant). The cartilage phenotype was not observed with control MO.

Depletion of p120 affects specific endogenous cadherin levels

Recent studies in cell lines have shown that binding of p120 may be important to stabilizing the E-cadherin protein (Ireton et al., 2002), and that it can regulate the turnover of cadherins in general (Davis et al., 2003; Xiao et al., 2003). To evaluate these observations in an embryonic context, we analyzed cadherin expression in embryos injected at the 1-cell stage with p120 MO. Immunoblot analysis of embryonic lysates isolated at different developmental stages revealed that p120 levels were moderately reduced at early gastrula stage (stage 10) and considerably at neurula (stage 15) and the tailbud (stage 22) stages [Fig. 4A, see also Table S1 in Supplemental data (http://jcs.biologists.org/cgi/content/full/117/18/4325/DC1)]. We noticed that depletion of p120 decreased the expression levels of C-

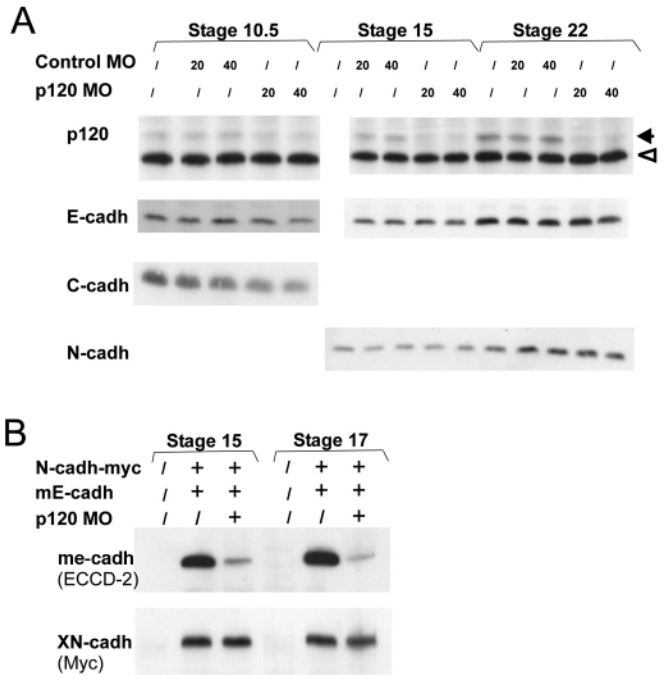

Fig. 4. Knockdown of p120 expression results in the downregulation of C- and E-cadherin proteins but not of N-cadherin. (A) An amount of 20 ng or 40 ng of control MO or p120 MO was injected at the 1-cell stage. Embryos were lysed at stages 10.5, 15 and 22 and analyzed for expression of p120 and C-, E- and N-cadherin. Injection of p120 MO leads to a dose-dependent downregulation of p120 (arrow). The strong band indicated by the open arrowhead is nonspecific and serves as a loading control. Next to a loss of p120 expression, lower levels of C-cadherin and E-cadherin can be observed. Levels of N-cadherin are not affected. (B) RNA (500 pg) encoding mE-cadherin or Myc-tagged XN-cadherin was injected at the 1-cell stage together with control MO or p120 MO (20 ng). Embryos were lysed at stages 15 and 17 and analyzed for expression of ectopic mE-cadherin and Myc-tagged XN-cadherin. While the expression levels of mE-cadherin are dramatically reduced upon the co-injection of p120 MO, the levels of ectopic XN-cadherin are not affected.

cadherin considerably, while E-cadherin protein was moderately reduced at the highest concentration of p120 MO and only at early gastrula stage. Interestingly, the levels of N-cadherin were not affected (Fig. 4A). The co-injection of p120 MO also strongly decreased the expression level of ectopic mouse E-cadherin, but not Myc-tagged *Xenopus* N-cadherin in *Xenopus* embryos (Fig. 4B). Because the cadherins are injected as synthetic RNA, the suppression of cadherin expression by p120 depletion must occur at the post-transcriptional level. The more potent effect of p120 depletion on ectopic versus endogenous E-cadherin suggests that p120 levels may be more rate limiting for ectopic (and overexpressed) cadherin than for endogenous cadherin protein.

The decrease in C- and E-cadherin protein induced by p120 MO was clearly not sufficient to induce any effect in a blastomere adhesion assay (data not shown). Neither did it affect the re-integration of transplanted aggregates in the blastocoel roof assay (data not shown). Both of these assays have been used before to demonstrate modulations in cadherin-dependent adhesion (Brieher and Gumbiner, 1994; Wacker et al., 2000). Taken together, p120 depletion appears to affect the expression levels of endogenous or ectopic E- and C-cadherin, while the levels of N-cadherin are not affected.

Expression of p120-uncoupled or JMD-deleted E-cadherin mutants also affects the eyes and the craniofacial skeleton

The highly conserved JMD of classical cadherins is crucial for the modulation of N-cadherin-mediated cell-cell adhesion during *Xenopus* embryogenesis (Kintner, 1992). As p120 interacts with the JMD, it can be considered the major candidate molecule for regulating the function of cadherins. A minimal core region within the JMD of E-cadherin is responsible for binding to p120 (Thoreson et al., 2000). To address the importance of p120 binding to the functionality of cadherins during early embryonic development, we generated two p120-uncoupled *Xenopus* E-cadherin variants, XE-cadh750AAA and XE-cadh753AAA, by mutating either the conserved amino acid residues 750-753 (GGG) or 753-756 (EED) of the XE-cadherin JMD to a triplet of alanines (AAA). The corresponding mutations in human E-cadherin disrupt the interaction with p120 either completely (by hE-cadh764AAA) or to a large extent (by hE-cadh761AAA) (Thoreson et al., 2000). Dorsal-animal overexpression of these two E-cadherin mutants induced defects in the eyes and the craniofacial skeleton similar to those observed upon injection of p120 MO (Fig. 5A,B and Table 3). However, the reduction of the eyes in embryos injected with the p120-uncoupled point mutants

Table 2. Percentages of the eye phenotype scored after injection of p120 MO

	% Normal	% Mild eye phenotype*	% Severe eye phenotype*	Total scored (n)	No. of experiments
Control MO (8.33 ng-16.65 ng)	90	10	0	60	4
p120 MO (8.33 ng-16.65 ng)	4	16	80	103	11
+10 pg p120iso1	3	62	35	31	1
+20 pg p120iso1	0	77	23	30	1
+30 pg p120iso1	90	10	0	48	1
+33 pg DN-Rac	42	46	12	56	3
+33 pg CA-Rac	5	28	67	20	1
+125 pg WT-RhoA	26.5	26.5	47	32	4
+45 pg DN-RhoA	8	27	65	26	1
+500 pg DN-LIMK	24	74	2	59	2
+150 pg CA-ROCK	15.5	61	23.5	26	2

*Mild eye phenotype, one or two eyes are substantially smaller; severe eye phenotype, one eye is absent or only rudiments are visible.

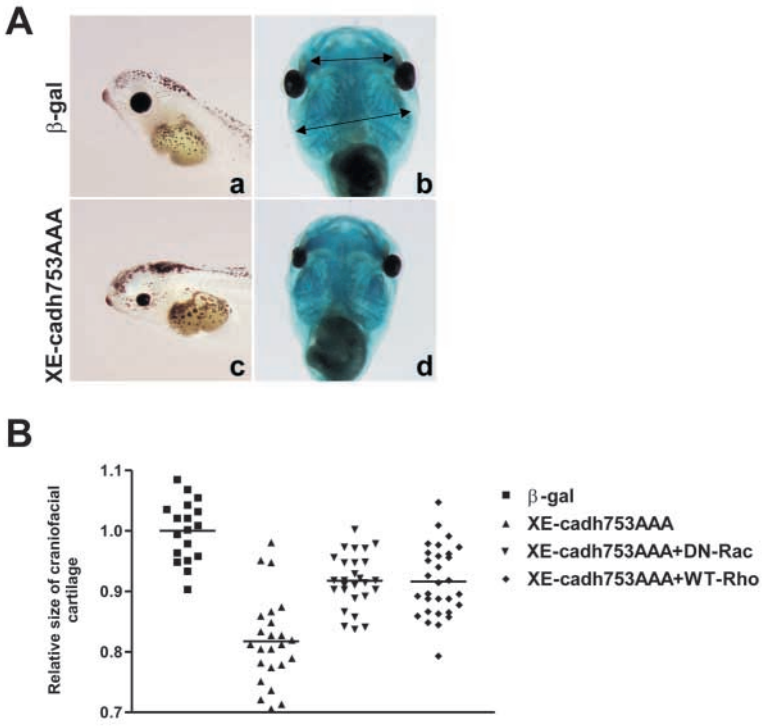

Fig. 5. Expression of p120-uncoupled E-cadherin affects the size of the eyes and cartilage. (A) Embryos were injected at the 8-cell stage in the dorsal-animal region and scored at stage 42 for the eye phenotype (a,c) and stage 46 for the cartilage phenotype after Alcian Blue staining (b,d). Tadpoles injected with 2 ng XE-cadh753AAA showing one smaller eye (c,d) compared with control injected embryos (a,b). (B) Graph representing the effect of XE-cadh753AAA RNA on the size of the craniofacial cartilage. Three normalized experiments are represented in one graph. The size of the head was calculated as in the legend of Fig. 3. The effect of XE-cadh753AA can be partially rescued by co-injection of 150 pg wild type (WT) RhoA or 50 pg dominant negative (DN) Rac (values are statistically different from those injected with XE-cadh753AAA RNA alone).

was less pronounced compared with embryos injected with p120 MO, in which the eyes were considerably smaller or even absent. Importantly, the eye and craniofacial malformations induced by XE-cadh753AAA could be rescued by the co-injection of wild-type XE-cadherin (data not shown).

Immunoblot analysis revealed that the injected p120-uncoupled XE-cadherin point mutants were poorly expressed in *Xenopus* (data not shown). It is also difficult to evaluate the ectopic expression levels, because the point-mutated XE-cadherins have the same molecular weight as the endogenous protein. To circumvent these problems, we decided to express mouse E-cadherin constructs ectopically in *Xenopus* embryos. We injected either full-length (FL) mE-cadherin or a mutant (mE-cadhΔJMD) with a 31 amino acid deletion that removes most of the JMD, including the p120 binding site and the tyrosine residues suspected of involvement in Hakai-mediated degradation (Fujita et al., 2002).

Expression in cell lines showed that this mutant is stable, functionally active and associates with α, β and γ catenins (Ozawa et al., 1990), but does not bind to p120 (data not shown). Surprisingly, embryos targeted in any region with ectopic FL mE-cadherin were phenotypically indistinguishable from noninjected controls, except for the dorso-vegetal zone where it induced ventralization by soaking up β-catenin. In contrast to FL E-cadherin, we observed that injection of equivalent amounts of mE-cadhΔJMD into the dorso-animal blastomeres resulted in prominent aberrations in the embryos, including severe malformations of the eyes (Fig. 6A). These malformations were, however, clearly different from those in embryos injected with Xp120 MO or with RNA encoding p120 or the p120-uncoupled XE-cadherin mutants. Instead of being reduced in size, the eyes were very irregularly shaped and patches of retinal pigmentation could often be observed within the brain (arrowhead in Fig. 6A).

When embryos injected with mE-cadhΔJMD were grown to stage 45-47, we observed that the majority developed with narrower heads, similar to embryos injected with p120 MO or with RNA encoding either XE-cadh750AAA or XE-cadh753AAA (Fig. 6B). Depending on the experiment, from 20 to 100% of the tadpoles that were injected with mE-cadhΔJMD showed more severe malformations of the jaw, manifested by protrusion of the interceratohyal muscle and the lower jaw, which resulted in a permanently open mouth. Interestingly, this defect could be fully rescued by coexpressing wild-type XE-cadherin or mE-cadherin (data not shown). Alcian Blue staining of the cartilage structures of tadpoles injected with p120 MO or mE-cadhΔJMD showed that all cranial structures were apparently normal (Fig. 7 and data not shown). All the structures that are derived from the three main streams of the cranial neural crest cells (i.e. the mandibular, the hyoid and the branchial stream) were present. However, we observed reduced thickness and rigidity of the structures, especially in the ceratohyal cartilage, which is derived from the hyoid stream of NCCs, and in the ceratobranchials, which are derived from the branchial stream.

These results demonstrate that p120 depletion, and expression of p120-uncoupled and JMD-deleted E-cadherin, disturb the formation of the eyes and the craniofacial cartilage structures.

Table 3. Percentages of eye phenotype scored after RNA injection

Injected RNA	% Normal	% Eye phenotype	Total scored (n)	No. of experiments
β-gal (2 ng)	99	1	100	4
XE-cadh750AAA (2 ng)	73	27	70	2
XE-cadh753AAA (2 ng)	35.5	64.5	101	6
+150 pg WT-Rho	83.5	16.5	95	6
+50 pg DN-Rac	88	12	91	5
+500 pg DN-LIMK	73.5	26.5	67	2
DN-RhoA (50 pg)	25	75	91	4
WT-RhoA (150 pg)	98	2	88	4
CA-RhoA (50 pg)	96	4	87	4
DN-Rac (50 pg)	97	3	68	3
CA-Rac (50 pg)	39	61	64	3
DN-LIMK (500 pg)	83	17	42	2

Depletion of p120 and overexpression of JMD-mutated E-cadherin disrupt morphogenetic movements in the anterior neural plate and cranial neural crest cell migration

The formation of the eyes starts with the induction of the retinal

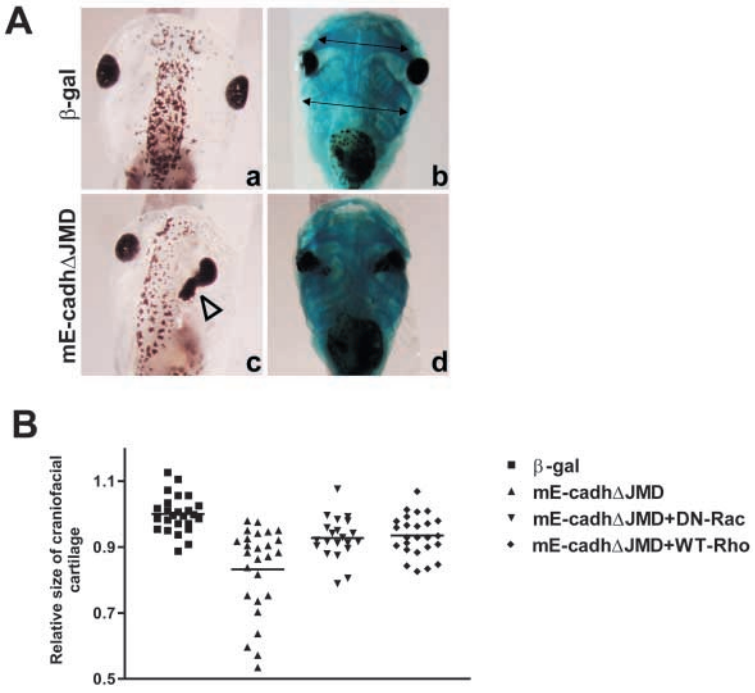

Fig. 6. Expression of JMD-deleted E-cadherin affects the eyes and cartilage. (A) Embryos were injected at the 8-cell stage in the dorsal-animal region and scored at stage 42 for the eye phenotype (a,c) and stage 46 for the cartilage phenotype after Alcian Blue staining (b,d). Embryos injected with 1 ng mE-cadhΔJMD show malformation of the eye (c,d) compared with control injected embryos (a,b). The arrowhead in (b) indicates a patch of retinal pigmentation in the brain. (B) Graph representing the effect of mE-cadhΔJMD on the size of the craniofacial cartilage. Three normalized experiments are represented in one graph. The width of the head was calculated as in the legend of Fig. 3. The effect of mE-cadhΔJMD can be partially rescued by co-injection of 150 pg wild type (WT) RhoA or 50 pg dominant negative (DN) Rac (values are statistically different from those injected with mE-cadhΔJMD RNA alone).

field in the anterior neural plate. After closure of the neural tube, the eye vesicles evaginate from the brain and induce lens formation where they contact the ectoderm. To evaluate the morphogenetic movements in the anterior neural plate directly in vivo, we co-injected one dorsal-animal blastomere of a 32-cell stage embryo with Rhodamine-dextran and control MO, p120 MO or mE-cadhΔJMD RNA. At stage 21 we could easily visualize the evaginating eye vesicle (arrowheads in Fig. 8A, panel d). However, these structures were not clearly delineated in embryos injected with p120 MO or with mE-cadhΔJMD RNA (Fig. 8A, panels e,f). Sections through the head region of embryos at stage 21 indicate that the evaginating eye vesicles are clearly visible in embryos injected with control MO (Fig. 8B, panels a,b). In contrast, these structures cannot be clearly distinguished in p120 MO-injected embryos (Fig. 8B, panels e,f) and are malformed in embryos injected with mE-cadhΔJMD RNA (Fig. 8B, panels i,j). In addition, it is clear that in p120 MO-injected embryos the anterior neural tissues had not separated properly from the overlying ectoderm, which may also correlate with the open neuropore (see end of this paragraph). At later stages of development, Rhodamine staining was clearly concentrated in the retinal cup of control MO-injected embryos, but spread out in embryos injected with p120 MO or mE-cadhΔJMD (Fig. 8A, panels g-l). Interestingly, if a small eye was formed, Rhodamine staining often surrounded the retinal cup (data not shown). Sections through the head region of stage 39 embryos show the smaller and under-developed eyes in p120 MO-injected embryos (Fig. 8B, panels g,h), while the retinal layers of tadpoles injected with mE-cadhΔJMD RNA are nicely stratified but show an aberrant shape and are not well separated from the brain (Fig. 8B, panels k,l). These results indicate that eye formation is affected at the earliest stages, most likely by impaired evagination of the retinal vesicle. While both p120 MO and mE-cadhΔJMD RNA injection affect the formation of the eye vesicles, there are clearly specific differences in the induced malformations. We noticed, for instance, that in embryos injected with p120 MO, the folding of the anterior neural rims was affected (Fig. 8A, arrowheads in panel b). Normally, the anterior folds of the neural plate form a loop, which gradually constricts and finally closes. This loop structure was often interrupted or not present in the p120 MO-injected embryos, and consequently the anterior neuropore stayed open for a longer time (Fig. 8A, arrow in panel e). Ultimately, however, the neural tube always closed by some alternative mechanism. Interestingly, we did not observe the same abnormal morphogenetic behaviors in embryos injected with mE-cadhΔJMD. Although the anterior neural rim was sometimes affected (Fig. 8A, arrowhead in panel c), closure of the anterior neuropore was normal.

The craniofacial cartilage is derived from the cranial NCCs that emigrate from the dorsal hindbrain into the branchial arches (Helms and Schneider, 2003). The reduced width and thickness of the cartilage structures of embryos injected with p120 MO, or with the p120-uncoupled or JMD-deleted cadherins, can be explained by impaired migration of the neural crest from the neural tube into the branchial arches, or by a reduced proliferation and/or increased apoptosis rate of the cells after they have properly migrated to their final position. To evaluate the migratory behavior of the cranial NCCs directly in vivo, we co-injected p120 MO or mE-cadhΔJMD synthetic RNA with a photo-activatable form of Fluorescein coupled to dextran. At the early neurula stage, the Fluorescein was activated in the region where the forming cranial NCCs are located. The migration of these cells into the branchial arches was then followed in real time. While the three streams of cranial NCCs originating at the dorsal side of the neural tube were broad and extended to a very ventral position in 90% of the embryos injected with the control MO (59 scored in four experiments), these streams were clearly aberrant or reduced in 64% of the embryos injected with p120 MO (35 scored in four experiments) or in 86% of the embryos injected with mE-cadhΔJMD RNA (38 scored in three experiments) (Fig. 9A). Interestingly, histological analysis of mE-cadhΔJMD-injected embryos (which have the strongest cartilage phenotype) showed large clumps of cells at stage 26 that were either associated with, or in close proximity to, the neural tube (Fig. 9B). This suggests that either the NCCs are unable to delaminate from the neural tube or they are unable to disperse after delamination.

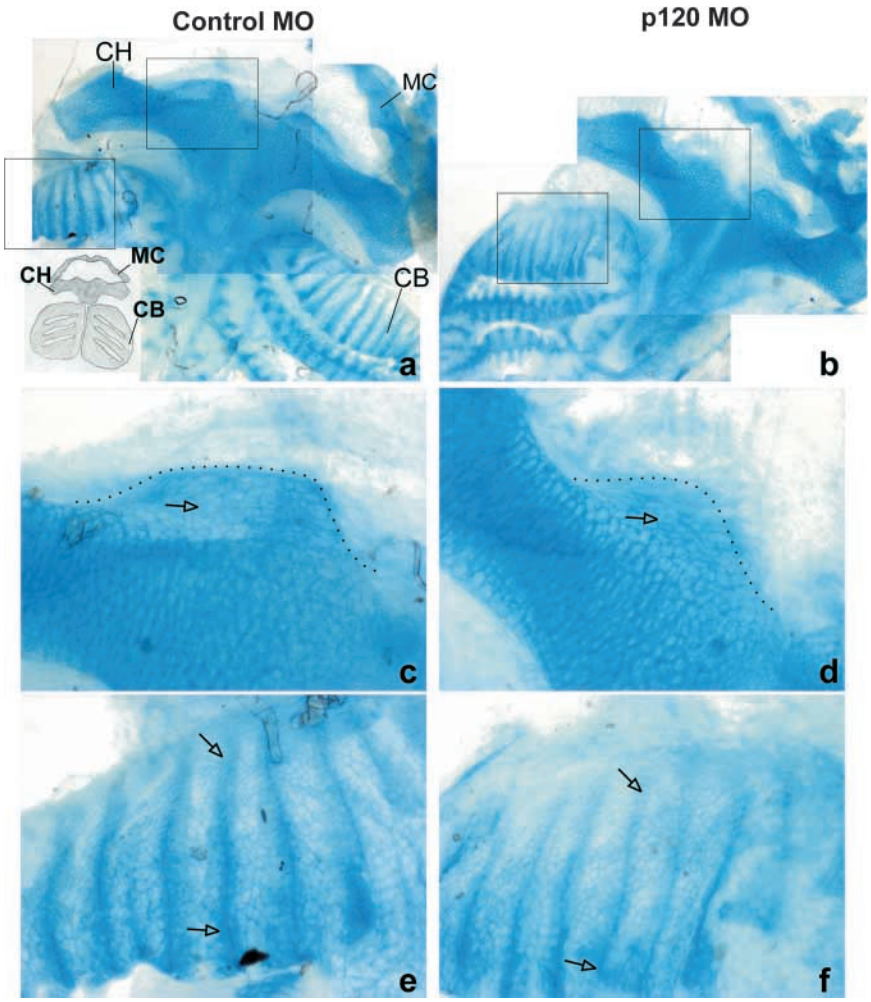

Fig. 7. Malformation of the jaws as a result of p120 depletion. Dissected craniofacial cartilage structures stained with Alcian Blue. The inset in (a) shows a schematic of the different craniofacial cartilage structures, including Meckel's cartilage (MC), ceratohyal (CH) and ceratobranchial cartilage (CB). All these structures are still present upon p120 knockdown (b) but are smaller compared with control MO-injected embryos (a). Boxed regions are enlarged in c-f. Higher magnification shows that the ceratohyal cartilage is less dense and delineated in embryos injected with p120 MO (d, see arrow and dotted line) compared with the same area in embryos injected with control MO (c). The same is true for the ceratobranchial cartilage (e,f), where the two arrows point out a ridge that is clearly less dense and composed of fewer cells in p120 MO-injected embryos.

In summary, the experiments with p120 MO and mE-cadhΔJMD RNA indicate that p120 and the JMD of cadherins are essential for the early stages of morphogenesis in the anterior neural tube, including the evagination of the eye vesicles, and for the proper migration of cranial NCCs into the branchial arches.

Dominant negative (DN) Rac1 and wild-type (WT) RhoA rescue the eye and craniofacial phenotypes

As it has been reported in the literature that expression of p120 in cell lines inhibits RhoA and activates Rac, we wondered whether a possible link exists between the observed eye and craniofacial malformations and the regulation of RhoA and Rac GTPases. Thus, we performed rescue experiments by injecting Xp120 MO, synthetic mRNA encoding p120-uncoupled, or JMD-deleted E-cadherin mutants, in combination with either wild type or mutant forms of RhoA and Rac1. Strikingly, coexpression of dominant negative (DN) Rac rescued all the eye and craniofacial phenotypes, whether induced by depletion of p120 (Fig. 3B, Tables 2, 3) or by expression of p120-uncoupled and JMD-deleted E-cadherin mutants (Fig. 5B, Fig. 6B, Table 3 and data not shown). Wild-type (WT) RhoA always had a less-effective rescuing activity than DN Rac and did not significantly rescue the craniofacial malformations induced by p120 MO and the eye phenotype of the JMD-deleted E-cadherin mutant. Interestingly, single injection of DN RhoA or constitutively active (CA) Rac1 strongly affected the anterior structures of the embryos, most notably the eyes (Table 3) and the craniofacial skeleton (data not shown).

To investigate the involvement of Rho GTPase activity in the observed phenotypes, we analyzed whether wild type or mutant versions of LIM kinase (LIMK) and Rho kinase (ROCK), known downstream effectors of the Rho GTPases that are described to be regulators of the actin cytoskeleton, would be able to rescue the phenotypes induced by p120 depletion and by ectopic expression of XE-cadh753AAA or mE-cadhΔJMD (Tables 2, 3 and data not shown). We found that a constitutively active form of ROCK seriously affected the gastrulation movements. DN ROCK, wild type (WT) and DN LIMK had no major effect on development. Interestingly, DN LIMK could rescue the eye and craniofacial phenotypes induced by p120 MO (Table 2 and Fig. 3B), XE-cadh753AAA and mE-cadhΔJMD RNA (Table 3 and data not shown). Consistent with the results obtained with WT RhoA, we noticed that CA ROCK was less potent in rescuing the eye and craniofacial phenotypes induced by p120 MO (Table 2, Fig. 3B and data not shown).

Dominant negative (DN) Rac1 and wild-type (WT) RhoA affect the localization and activity of cadherins in the embryo

To examine how the Rho GTPases execute their rescue, we analyzed their effect on cadherin expression and localization in migrating cranial NCCs. The lack of proper antibodies to evaluate endogenous cadherins involved in the morphogenetic phenotypes prompted us to evaluate the effects of the Rho GTPases on the ectopic mE-cadherin, for which good antibodies for immunohistochemistry are available. We co-injected mE-cadhΔJMD, which on its own generates severe eye and craniofacial perturbations, with rescuing concentrations of WT

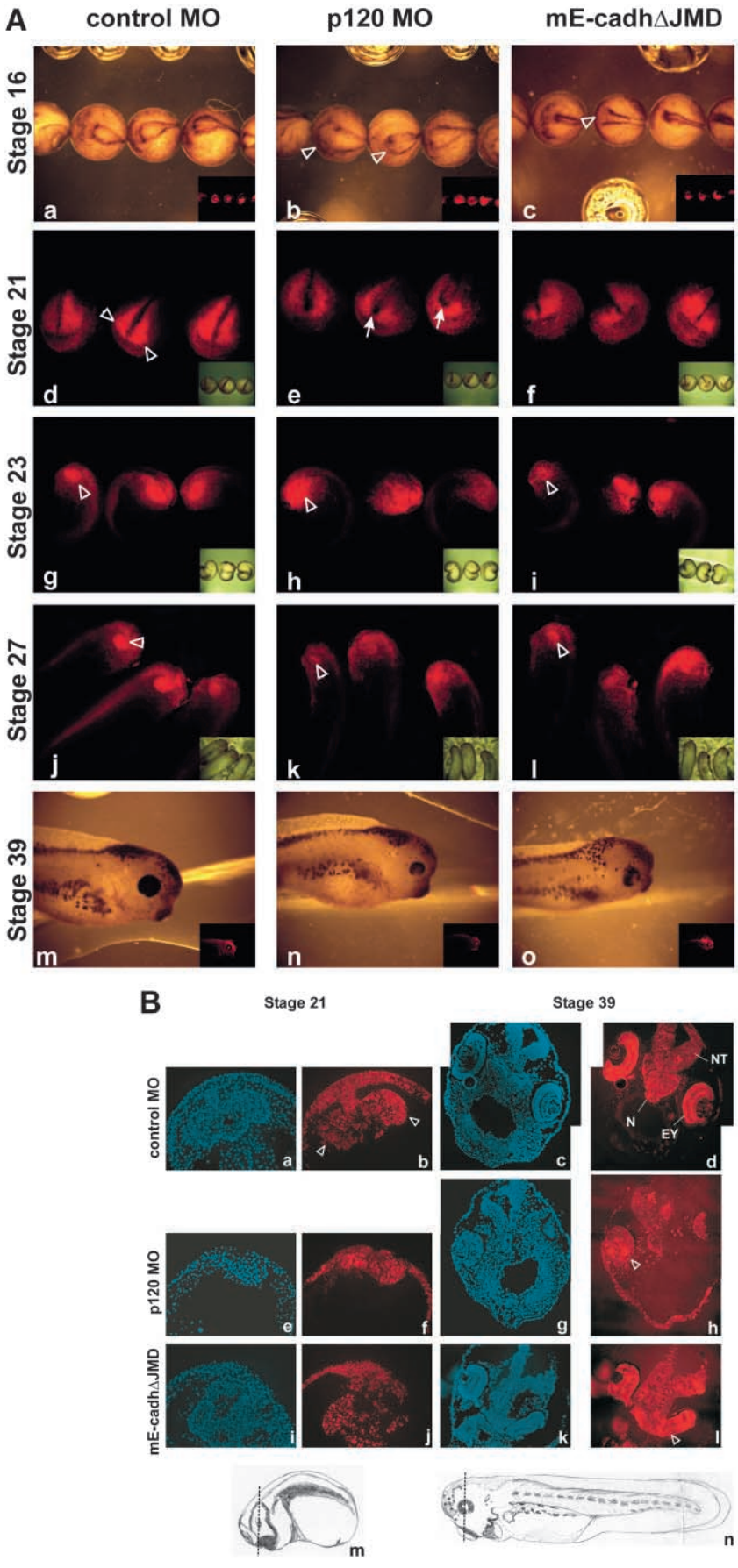

Fig. 8. Abnormal evagination of the eye vesicles in embryos injected with p120 morpholino (MO) or RNA encoding JMD-deleted E-cadherin. (A) Embryos were injected at the 32-cell stage with Rhodamine-dextran and MO or RNA in two blastomeres in the region that contributes to the eye. At stage 16, knockdown of p120 leads to defects in the anterior loop structure of the closing neural tube (b, arrowheads). This can also be observed in a minority of embryos injected with mE-cadhΔJMD (c, arrowhead) but not in embryos injected with control MO (a). At stage 21 the evagination of the eye has clearly started in control MO-injected embryos (d, see arrowheads). In embryos injected with p120 MO (e) and mE-cadhΔJMD RNA (f) this process is disturbed. At this stage the anterior neuropore of p120 MO-injected embryos is still open (arrow in e). At early and late tailbud stages (stages 23 and 27) the control MO-injected embryos show a nicely formed eye (g,j, see arrowheads) compared with the p120 MO-injected embryos (h,k, see arrowheads). Expression of mE-cadhΔJMD also leads to a disturbance of the eyes at early and late tailbud stages (i and l, see arrowheads). At stage 39, control MO-injected embryos show nicely formed eyes (m), compared with p120 MO-injected embryos, which exhibit smaller eyes (n), or mE-cadhΔJMD injected embryos, which have malformed eyes (o). (B) Transverse sections of Rhodamine-injected and DAPI stained embryos at stage 21 and 39. At stage 21, the embryos injected with control MO show a good evagination of the eye vesicles from the neural tube (a,b, see arrowheads). This morphogenetic process is clearly aberrant in embryos injected with p120 MO (e,f) or mE-cadhΔJMD (i,j) (see text for details). A schematic indicating the site of the section is shown in (m). At stage 39 embryos injected with control MO have eyes with a proper stratification of the retinal layers (c,d). The brain or neural tube (NT), the notochord (N) and the eyes (EY) are indicated. Eyes are smaller and the retinal stratification is lost in embryos injected with p120 MO (g,h, see arrowhead). Embryos expressing mE-cadhΔJMD show stratification of the retina, but the eyes are malformed and are not well separated from the brain (k,l, see arrowhead). A schematic indicating the site of the section is shown in (n).

RhoA and DN Rac, and analyzed ectopic cadherin expression and localization in the migrating cranial NCCs. Whereas mE-cadhΔJMD is strongly expressed and evenly distributed in NCCs when injected alone (Fig. 10A, panels a and d), its localization was more scattered in NCCs coexpressing DN Rac (Fig. 10A, panels b,e), and mE-cadhΔJMD protein levels were reduced when WT RhoA was coexpressed (Fig. 10A, panels c,f). This suggests that DN Rac, and to a lesser extent WT RhoA, can reduce the intercellular adhesiveness between the cranial NCCs, and hence facilitate the emigration of this cell population from the neural tube and its migration into the branchial arches.

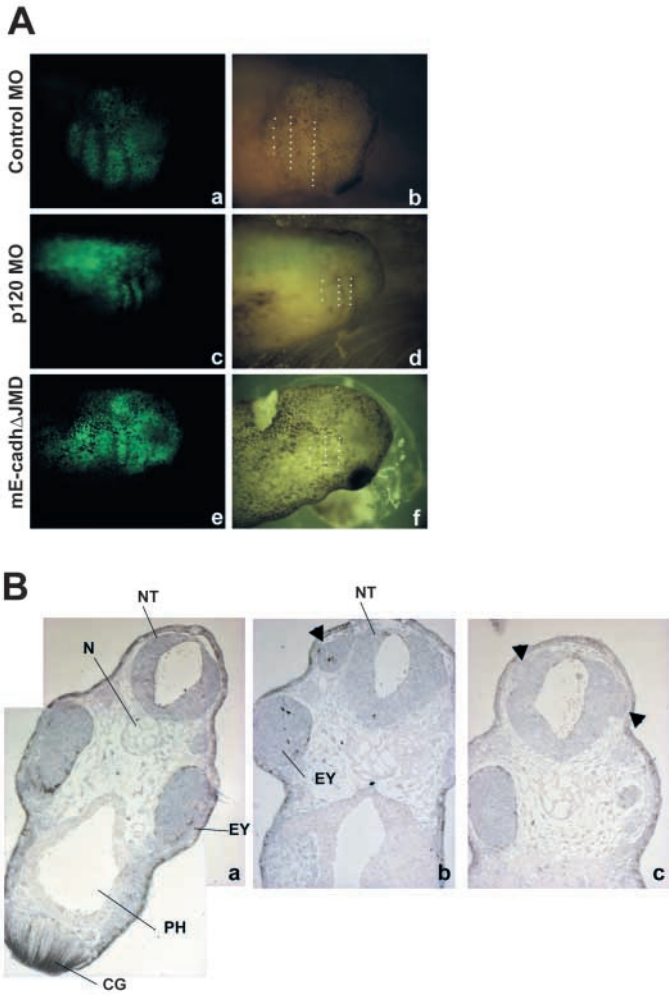

Fig. 9. Disturbance of cranial neural crest cell (NCC) migration upon injection of p120 morpholino (MO) or RNA-encoding JMD-deleted E-cadherin. (A) Tracing of cranial NCCs migrating into the branchial arches. Embryos were injected at the 4-cell stage with caged Fluorescein-dextran in combination with control MO (a,b), p120 MO (c,d) or mE-cadhΔJMD RNA (e,f). At stage 14, the Fluorescein was activated with UV light in the region where the NCCs originate. Embryos injected with control MO show the three wide streams of migrating cranial NCCs (a,b). Depletion of p120 (c,d) or overexpression of mE-cadhΔJMD (e,f) leads to disturbance in the migration of the NCCs. The three streams do not go as deep as in the control MO-injected embryos and they are not as wide (c,d and e,f, respectively). Dotted lines (b,d and f) show a projection of the three streams (a,c and e, respectively). (B) Transverse histological sections of the head of stage 26 embryos. Embryos were injected with mE-cadhΔJMD at the 4-cell stage and fixed for sectioning at stage 26. Transverse section of the head of a non-injected embryo (a), showing the neural tube (NT), the notochord (N), the eyes (EY), the pharynx (PH) and the cement gland (CG). Embryos injected with mE-cadhΔJMD (b,c) show clumps of intimately associated cells in close proximity to the neural tube or still attached to the neural tube (arrowheads).

We also wanted to analyze whether DN Rac and WT RhoA affect the association of mE-cadhΔJMD with α-catenin. For this we co-injected a plasmid encoding a chimeric fusion of αE-catenin and EGFP, which can be evaluated directly in vivo under a confocal laser scanner microscope. Because the plasmid is unevenly distributed between the cells with successive cell divisions, the injected plasmid generates mosaic expression of the EGFP fusion protein in the developing embryos. Consequently, we noticed various expression levels of αE-catenin-EGFP. Because of the limited transparency of the *Xenopus* embryos at the earlier developmental stages, we could only evaluate the localization of the fusion protein in the outer cell layers and not in the NCCs. We noticed that αE-catenin-EGFP is clearly localized at cell-cell contacts in control-injected embryos (Fig. 10B, panel a). Strikingly, when mE-cadhΔJMD was co-injected, strong enrichment of αE-catenin-EGFP proteins was visible at cell-cell contacts (Fig. 10B, panel b). The intercellular contacts mostly formed straight lines, suggesting that cortical tension is strong and cells are robustly associated. We also noticed a higher tendency for cells coexpressing the αE-catenin-EGFP and mE-cadhΔJMD to be grouped together, while they were more dispersed in control injected embryos. This suggests that cells derived from the same precursor stay more associated in embryos injected with mE-cadhΔJMD than in control-injected embryos. When DN Rac was co-injected with mE-cadhΔJMD, the concentration of αE-catenin-EGFP was greatly reduced (Fig. 10B, panel c), and the evaluation of different Z-sections revealed that its localization at cell-cell contacts was limited to a fine line (data not shown). Conversely, the co-injection of WT RhoA had no effect on the localization of αE-catenin-EGFP.

Taken together, the microscopic analysis of sections and the in vivo experiments suggest that DN Rac affects the concentration of cadherin at the membrane, and has a strong influence on the interaction of cadherins with α-catenin. Whereas, WT RhoA primarily seems to change the expression and/or function of the cadherin, while the association with α-catenin is not affected.

Discussion

Studies in cell lines indicate that p120 is ideally positioned to transfer signals from the cadherins to the cytoskeleton (outside-in signaling), and to transmit intracellular signaling events that influence the activity and/or expression levels of the cadherin at the membrane (inside-out signaling). While studies in *C. elegans* and *Drosophila* have indicated that p120 is dispensable for development in invertebrates, it was shown recently that p120 is an essential factor in vertebrate development, and is required for normal gastrulation and convergent extension movements (Fang et al., 2004). In our study we documented an essential role for p120 in the morphogenetic movements associated with the formation of the eyes and the craniofacial skeleton and analyzed the molecular mechanism by which p120 exerts this control.

Our data indicate that p120 is involved in regulating morphogenesis in early *Xenopus* embryos, especially in derivatives of the ectodermal cell lineage. Firstly, we demonstrate that while basal levels of p120 transcripts are expressed throughout the embryo, mRNA expression is particularly enriched in embryonic regions that undergo extensive morphogenetic movements. This is especially true for tissues, such as the head (neuro)ectoderm, the eye vesicles and the cranial neural crest, a highly migratory cell population that originates at the border of the anterior neural plate and the future epidermis. Secondly, we show that morpholino (MO)-

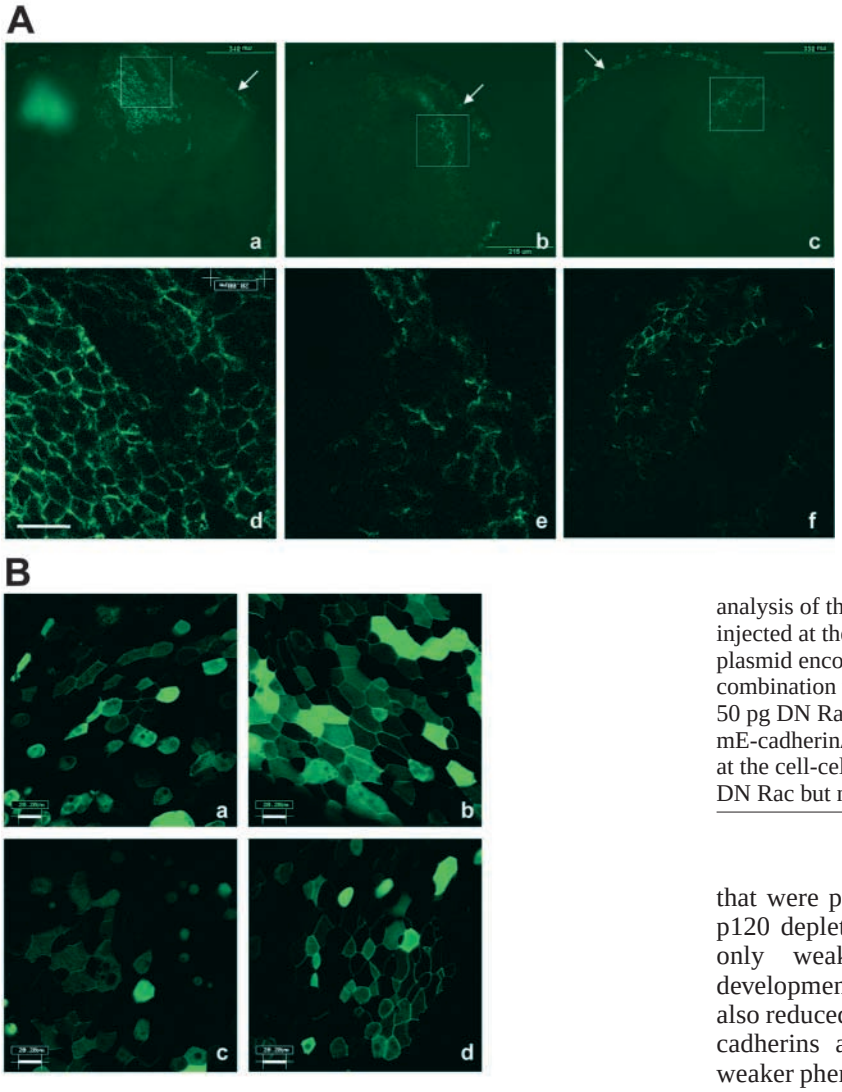

Fig. 10. Localization of JMD-deleted E-cadherin and αE-catenin-EGFP in fixed and living embryos. (A) Immunohistological examination of mE-cadhΔJMD expression in transverse sections of stage 21 embryos. Embryos were injected at the 16-cell stage and fixed for sectioning at stage 21. After sectioning, immunohistochemical staining was performed to localize mE-cadherinΔJMD proteins, and sections were examined with a fluorescence (a-c) or a laser scanner confocal microscope (d-f). Embryos injected with mE-cadhΔJMD (500 pg) alone show a high and uniform concentration of mE-cadherinΔJMD at the cell-cell contacts in the cranial NCCs (a,d). Expression of mE-cadherinΔJMD in embryos co-injected with dominant negative (DN) Rac (50 pg) is more scattered (b,e) while an overall reduced staining is observed upon co-injection of 150 pg wild type (WT) RhoA RNA (c,f). All sections are oriented with dorsal side up. Staining in the ectoderm is indicated by an arrow, and the boxed area in the migrating neural crest cells is examined by confocal microscopy. Scale bar, 20 μm. (B) Confocal in vivo analysis of the ectodermal cell layer in tailbud-stage embryos injected at the 16-cell stage in the ventral-animal region with a plasmid encoding αE-catenin-EGFP alone (a) or with the plasmid in combination with 500 pg mE-cadhΔJMD RNA (b) and additionally 50 pg DN Rac (c) or 150 pg WT RhoA RNA (d). While injection of mE-cadherinΔJMD induces strong localization of αE-catenin-EGFP at the cell-cell contacts, this is greatly reduced upon co-injection of DN Rac but not by WT RhoA. Scale bars, 20 μm.

mediated depletion of p120 affects the formation of the eyes and the craniofacial skeleton, structures that are derived from tissues in which p120 messenger is highly enriched, i.e. the eye vesicle and the cranial neural crest. Thirdly, using in vivo labeling techniques, we show that the evagination of the eye vesicles from the brain is disturbed in p120-depleted embryos, as is the migration of the cranial NCCs from the dorsal side of the neural tube into the branchial arches.

We found that depletion of p120 decreased the endogenous or ectopic levels of C- and E-cadherin proteins, which is consistent with recent reports describing similar effects of p120 in cell culture (Davis et al., 2003; Xiao et al., 2003) and in *Xenopus* embryos (Fang et al., 2004). However, N-cadherin levels were not affected. This may correlate with the presence of one or two of the tyrosine residues suspected in Hakai-mediated degradation in C- and E-cadherin, respectively, and their absence in N-cadherin (Fujita et al., 2002). Presently, however, it is not clear whether the reduced C- and E-cadherin levels are related to the observed malformations in the eyes and the craniofacial skeleton, whose progenitors presumably do not even express C- or E-cadherin.

Interestingly, we could phenocopy the eye and craniofacial malformations by overexpression of XE-cadherin derivatives that were point mutated in the p120 binding site. Similar to p120 depletion, these cadherin mutants, which no longer or only weakly bind p120, reproducibly affected eye development, albeit less prominently than p120 MO. They also reduced the width of the head. We found that these mutant cadherins are poorly expressed, which may explain their weaker phenotype. Dorso-animal expression of a mE-cadherin derivative that contains a 31 amino acid deletion in the JMD, covering both the p120 and the Hakai-binding sites, affected the formation of the eyes and the craniofacial cartilage more severely. However, in this case the eye phenotype was clearly different from that obtained after p120 depletion or expression of a p120-uncoupled point mutated E-cadherin. Rather than being reduced in size or totally absent, the eyes were very irregularly shaped, and retinal pigmentation could often be observed in the optic stalk and in patches of cells that were located within the brain. Because the JMD-deleted E-cadherin mutant is more strongly localized at cell-cell contacts compared with full length E-cadherin, the phenotypes could be explained by the inability of some cells to turn down cadherin expression or functionality. Evidently, because a 31 amino acid region is missing from this mutant, binding to components other than p120 and Hakai may be disrupted. This may prevent dynamic regulation of this cadherin, which is necessary for the correct morphogenetic movements associated with eye and jaw formation. The malformations of the craniofacial skeleton were most severe for this deletion mutant. In addition to being smaller, the lower jaws had malformations severe enough to prevent closing of the mouth. Microscopic inspection of the alcian-blue-stained craniofacial cartilage skeleton indicated a greatly reduced number of cells

in these structures in embryos injected with p120 MO or with the JMD-deleted E-cadherin.

In vivo labeling of specific cell populations in embryos injected with p120 MO or JMD-deleted E-cadherin indicated that both the correct evagination and/or proximal constriction of the eye vesicle were affected, and the migration of the cranial NCCs was reduced. This indicates that the small eyes and the reduced craniofacial cartilage structures are primarily the result of impaired morphogenetic behavior, and not of defects in cell proliferation and/or specification. We also observed that p120 MO, and to a lesser extent JMD-deleted E-cadherin, affected the structure of the anterior neural folds, which caused aberrant closure of the anterior neural plate. It is possible that apical cellular constrictions, which are probably needed to allow the correct formation of the neural ridges and the infolding of the anterior neural tube, are disturbed by p120 depletion. Importantly, we observed that upon injection of p120 MO or the p120-uncoupled E-cadherin point mutants, the eyes were always well separated from the brain, even when they were considerably reduced in size. Actually, we never observed cyclopia, which normally results from incomplete separation of the presumptive eye field in the anterior neural plate, and can be a sign of general ventralization of the embryo and/or deficient signaling from the prechordal plate that moves underneath the eye field and induces its separation. This indicates that the reduced size of the eyes does not result from changes in the anterior-posterior patterning of the embryo.

The impaired migration of the cranial NCCs depleted of p120 or expressing the JMD-deleted E-cadherin mutant raises the important question of why these cells are curtailed in their migratory behavior. This could be the result of impaired cell-cell adhesion, a failure of the NCCs to respond to the migratory cues in the tissues they have to transverse, or in the light of our results with the Rho GTPases (see next paragraph), from a cytoskeletal condition unsupportive of migration, or from a combination of any these processes. The JMD-deleted E-cadherin induced the strongest phenotype in the cranial cartilage, and histological inspection of the head region of embryos injected with the JMD-deleted E-cadherin mutant indicated the presence of tightly packed cells flanking the neural tube. These are probably NCCs that have delaminated but failed to disperse. Immunolabeling of cells expressing the JMD-deleted cadherin showed that these cells are tightly packed, and display continuously high concentrations of the cadherin at the intercellular contacts. This suggests, at least for cranial NCCs expressing the JMD-deleted E-cadherin, that intercellular adhesion is too robust or static to permit the efficient emigration of these cells from the dorsal neural tube region into the branchial arches. Our results also imply that NCCs, aside from changing cadherin patterns (Nakagawa and Takeichi, 1998; Pla et al., 2001), also need to suppress cadherins functionally to delaminate and migrate. This is in agreement with our observation that overexpressed wild-type mE-cadherin does not impair NCC migration, and actually competitively rescues the phenotype generated by the JMD-deleted E-cadherin. This is further in line with results in avian embryos, where it was shown that in migrating NCCs, N-cadherin is expressed, but is not located at the cell surface and is not connected to the cytoskeleton (Monier-Gavelle and Duband, 1995). Interestingly, inhibitors of protein kinases (including tyrosine kinases) restored N-cadherin-mediated cellular contacts and prevented migration. These results imply that NCCs possess a mechanism for suppressing N-cadherin function. The same mechanism may be responsible for the functional suppression of ectopically expressed wild-type E-cadherin in our experimental set-up, or it may regulate the activity of endogenous Xcadherin-11, which is the major cadherin expressed in the cranial NCCs of *Xenopus* and is involved in its migration and specification (Borchers et al., 2001).

Intriguing is the ability of dominant negative (DN) Rac, and to a lesser extent wild type (WT) RhoA, to rescue the phenotypes induced by p120 depletion, or by overexpression of the p120-uncoupled and JMD-deleted cadherin mutants. This implies that manipulation of Rho GTPase activity can relieve the restrictions imposed by these treatments. In line with these results, we found that DN RhoA and CA Rac also induce smaller eyes and heads. Because Rho GTPases have been implicated in various biological processes, including regulation of actin dynamics, cell adhesion, transcription, cell growth and membrane trafficking (reviewed by Etienne-Manneville and Hall, 2002), we can envision different scenarios by which Rho GTPases affect morphogenetic movements. However, several reports support a direct role for the Rho GTPases in cadherin-mediated cell adhesion, with the strongest case for the involvement of Rac (Fukata and Kaibuchi, 2001). Moreover, p120 has been shown to regulate cell motility through regulation of the Rho GTPases (Anastasiadis et al., 2000; Grosheva et al., 2001; Noren et al., 2000). The observation that DN LIMK, a downstream effector of Rac that plays a role in the regulation of the actin cytoskeleton, is also efficient in rescuing the eye and craniofacial phenotypes, hints that changes in the actin cytoskeleton are associated with the observed morphogenetic phenotypes. More experiments are needed to clarify the involvement of the Rho GTPases at the mechanistic level.

Our results do not allow us to draw unambiguous conclusions on how p120 depletion affects morphogenetic behavior in general and cadherin function in particular. Because part of the phenotypes of p120 depletion can be phenocopied by the expression of the p120-uncoupled and JMD-deleted cadherin mutants, and as the latter clearly increases intercellular contacts in the embryonic context, it is tempting to speculate that p120 depletion also reinforces cadherin-mediated adhesion in this experimental setting. This would also clarify the comparable rescuing activities of DN Rac, DN LIMK, WT RhoA and CA ROCK. Unfortunately, we currently lack the appropriate tools for investigating this scenario. In conflict with such a conclusion are, of course, recent reports that clearly show that p120 stabilizes cadherin expression, at least in cell lines (Davis et al., 2003; Xiao et al., 2003). It is, however, quite possible that this activity is dependent on the cellular context, and it has often been found that cells in a natural three-dimensional context acquire properties different from those developed when growing on an artificial substrate. In accordance with this, we clearly showed that in our experimental setup N-cadherin expression is not affected by p120 depletion. Hence, cell-cell adhesion exerted by N-cadherin or another cadherin (e.g. cadherin-11), may not be functionally suppressed in the morphogenetic tissues upon p120 depletion. Interestingly, mis-expression studies in *Xenopus* have shown that NCCs overexpressing either full

length cadherin-11, the major cadherin expressed in migrating NCCs in *Xenopus*, or a DN mutant lacking the β-catenin binding site, fail to migrate efficiently into the branchial arches (Borchers et al., 2001). This implies that both too much and too little adhesion affect the migration of these cells. Evidently, further research is needed to discover exactly how p120 depletion influences the different morphogenetic processes.

In conclusion, our work demonstrates that in contrast to invertebrates, p120 is essential for correct morphogenesis in vertebrate embryos. By acting directly on the activity of the cadherins at the membrane, and by signaling to the cytoskeleton, p120 may be a key factor that coordinates cell-cell adhesion with the activities of the cytoskeleton and the cell-substrate adhesion machinery.

We would like to thank H. Funakoshi, T. Nakamura, K. Kaibuchi, B. Janssens, A. Hall, M. Takeichi, B. Gumbiner, M. Ozawa and R. Kemler for their generous gifts of plasmids and antibodies. We are indebted to E. Parthoens for excellent support with confocal microscopy, to P. De Bleser for help with bioinformatics, to A. Servaes for aid throughout the project and to A. Cauwels and A. Bredan for critical reading and editorial assistance. Research is supported by grants from the Belgian Federation against Cancer and the Interuniversitaire Attractiepolen. M.D. and V.V. are fellows with the Institute for the Promotion of Innovation through Science and Technology in Flanders (IWT-Flanders). K.V. is a post-doctoral fellow with the FWO-Vlaanderen.

References

Aho, S., Rothenberger, K. and Uitto, J. (1999). Human p120(Ctn) catenin: tissue-specific expression of isoforms and molecular interactions with BP180 type XVII collagen. *J. Cell. Biochem.* **73**, 390-399.

Anastasiadis, P. Z. and Reynolds, A. B. (2000). The p120 catenin family: complex roles in adhesion, signaling and cancer. *J. Cell Sci.* **113**, 1319-1334.

Anastasiadis, P. Z., Moon, S. Y., Thoreson, M. A., Mariner, D. J., Crawford, H. C., Zheng, Y. and Reynolds, A. B. (2000). Inhibition of RhoA by p120 catenin. *Nat. Cell Biol.* **2**, 637-644.

Baki, L., Marambaud, P., Efthimiopoulos, S., Georgakopoulos, A., Wen, P., Cui, W., Shioi, J., Koo, E., Ozawa, M., Friedrich, V. L. et al. (2001). Presenilin-1 binds cytoplasmic epithelial cadherin, inhibits cadherin/p120 association, and regulates stability and function of the cadherin/catenin adhesion complex. *Proc. Natl. Acad. Sci. USA* **98**, 2381-2386.

Bellefroid, E. J., Bourguignon, C., Hollemann, T., Ma, Q., Anderson, D. J., Kintner, C. and Pieler, T. (1996). X-MyT1, a *Xenopus* C2HC-type zinc finger protein with a regulatory function in neuronal differentiation. *Cell* **87**, 1191-1202.

Borchers, A., David, R. and Wedlich, D. (2001). *Xenopus* cadherin-11 restrains cranial neural crest migration and influences neural crest specification. *Dev.* **128**, 3049-3060.

Braga, V. (2002). Cell-cell adhesion and signalling. *Curr. Opin. Cell Biol.* **14**, 546-556.

Brieher, W. M. and Gumbiner, B. M. (1994). Regulation of C-cadherin function during activin induced morphogenesis of *Xenopus* animal caps. *J. Cell Biol.* **126**, 519-527.

Chen, H., Paradies, N. E., Fedor-Chaiken, M. and Brackenbury, R. (1997). E-cadherin mediates adhesion and suppresses cell motility via distinct mechanisms. *J. Cell Sci.* **110**, 345-356.

Chen, X., Kojima, S., Borisy, G. G. and Green, K. J. (2003). p120 catenin associates with kinesin and facilitates the transport of cadherin-catenin complexes to intercellular junctions. *J. Cell Biol.* **163**, 547-557.

Davis, M. A., Ireton, R. C. and Reynolds, A. B. (2003). A core function for p120-catenin in cadherin turnover. *J. Cell Biol.* **163**, 525-534.

Etienne-Manneville, S. and Hall, A. (2002). Rho GTPases in cell biology. *Nature* **420**, 629-635.

Fang, X., Ji, H., Kim, S. W., Park, J. I., Vaught, T. G., Anastasiadis, P. Z., Ciesiolka, M. and McCrea, P. D. (2004). Vertebrate development requires ARVCF and p120 catenins and their interplay with RhoA and Rac. *J. Cell Biol.* **165**, 87-98.

Franz, C. M. and Ridley, A. J. (2003). p120ctn associates with microtubules: inverse relationship between microtubule binding and Rho GTPase regulation. *J. Biol. Chem.* **279**, 6588-6594.

Fujita, Y., Krause, G., Scheffner, M., Zechner, D., Leddy, H. E., Behrens, J., Sommer, T. and Birchmeier, W. (2002). Hakai, a c-Cbl-like protein, ubiquitinates and induces endocytosis of the E-cadherin complex. *Nat. Cell Biol.* **4**, 222-231.

Fukata, M. and Kaibuchi, K. (2001). Rho-family GTPases in cadherin-mediated cell-cell adhesion. *Nat. Rev. Mol. Cell Biol.* **2**, 887-897.

Geis, K., Aberle, H., Kuhl, M., Kemler, R. and Wedlich, D. (1998). Expression of the Armadillo family member p120cas1B in *Xenopus* embryos affects head differentiation but not axis formation. *Dev. Genes Evol.* **207**, 471-481.

Grosheva, I., Shtutman, M., Elbaum, M. and Bershadsky, A. D. (2001). p120 catenin affects cell motility via modulation of activity of Rho-family GTPases: a link between cell-cell contact formation and regulation of cell locomotion. *J. Cell Sci.* **114**, 695-707.

Gumbiner, B. M. (2000). Regulation of cadherin adhesive activity. *J. Cell Biol.* **148**, 399-404.

Helms, J. A. and Schneider, R. A. (2003). Cranial skeletal biology. *Nature* **423**, 326-331.

Ireton, R. C., Davis, M. A., van Hengel, J., Mariner, D. J., Barnes, K., Thoreson, M. A., Anastasiadis, P. Z., Matrisian, L., Bundy, L. M., Sealy, L. et al. (2002). A novel role for p120 catenin in E-cadherin function. *J. Cell Biol.* **159**, 465-476.

Keirsebilck, A., Bonné, S., Staes, K., van Hengel, J., Nollet, F., Reynolds, A. and van Roy, F. (1998). Molecular cloning of the human p120^{ctn} catenin gene (CTNND1): expression of multiple alternatively spliced isoforms. *Genomics* **50**, 129-146.

Kintner, C. (1992). Regulation of embryonic cell adhesion by the cadherin cytoplasmic domain. *Cell* **69**, 225-236.

Magie, C. R., Pinto-Santini, D. and Parkhurst, S. M. (2002). Rho1 interacts with p120ctn and alpha-catenin, and regulates cadherin-based adherens junction components in *Drosophila*. *Development* **129**, 3771-3782.

Marambaud, P., Shioi, J., Serban, G., Georgakopoulos, A., Sarner, S., Nagy, V., Baki, L., Wen, P., Efthimiopoulos, S., Shao, Z. et al. (2002). A presenilin-1/gamma-secretase cleavage releases the E-cadherin intracellular domain and regulates disassembly of adherens junctions. *EMBO J.* **21**, 1948-1956.

Mareel, M. and Leroy, A. (2003). Clinical, cellular, and molecular aspects of cancer invasion. *Physiol. Rev.* **83**, 337-376.

Monier-Gavelle, F. and Duband, J. L. (1995). Control of n-cadherin-mediated intercellular adhesion in migrating neural crest cells in vitro. *J. Cell Sci.* **108**, 3839-3853.

Moody, S. A. (1987). Fates of the blastomeres of the 32-cell-stage *Xenopus* embryo. *Dev. Biol.* **122**, 300-319.

Myster, S. H., Cavallo, R., Anderson, C. T., Fox, D. T. and Peifer, M. (2003). *Drosophila* p120catenin plays a supporting role in cell adhesion but is not an essential adherens junction component. *J. Cell Biol.* **160**, 433-449.

Nakagawa, S. and Takeichi, M. (1998). Neural crest emigration from the neural tube depends on regulated cadherin expression. *Development* **125**, 2963-2971.

Newport, J. and Kirschner, M. (1982). A major developmental transition in early *Xenopus* embryos: I. Characterization and timing of cellular changes at the midblastula stage. *Cell* **30**, 675-686.

Nieuwkoop, P. D. and Faber, J. (1994). *Normal table of Xenopus laevis (Daudin): a systematical and chronological survey of development from the fertilized egg till the end of metamorphosis*. New York, NY: Garland Science.

Noren, N. K., Liu, B. P., Burridge, K. and Kreft, B. (2000). p120 catenin regulates the actin cytoskeleton via Rho family GTPases. *J. Cell Biol.* **150**, 567-579.

Ozawa, M., Ringwald, M. and Kemler, R. (1990). Uvomorulin-catenin complex formation is regulated by a specific domain in the cytoplasmic region of the cell adhesion molecule. *Proc. Natl. Acad. Sci. USA* **87**, 4246-4250.

Pacquelet, A., Lin, L. and Rorth, P. (2003). Binding site for p120/delta-catenin is not required for *Drosophila* E-cadherin function in vivo. *J. Cell Biol.* **160**, 313-319.

Pasqualetti, M., Ori, M., Nardi, I. and Rijli, F. M. (2000). Ectopic Hoxa2 induction after neural crest migration results in homeosis of jaw elements in *Xenopus*. *Development* **127**, 5367-5378.

Paulson, A., Fang, X., Ji, H., Reynolds, A. B. and McCrea, P. D. (1999). Misexpression of the catenin p120(ctn)1A perturbs *Xenopus* gastrulation but does not elicit Wnt-directed axis specification. *Dev. Biol.* **207**, 350-363.

Perez-Moreno, M., Jamora, C. and Fuchs, E. (2003). Sticky business: orchestrating cellular signals at adherens junctions. *Cell* **112**, 535-548.

Pettitt, J., Cox, E. A., Broadbent, I. D., Flett, A. and Hardin, J. (2003). The *Caenorhabditis elegans* p120 catenin homologue, JAC-1, modulates cadherin-catenin function during epidermal morphogenesis. *J. Cell Biol.* **162**, 15-22.

Pla, P., Moore, R., Morali, O. G., Grille, S., Martinozzi, S., Delmas, V. and Larue, L. (2001). Cadherins in neural crest cell development and transformation. *J. Cell. Physiol.* **189**, 121-132.

Riehl, R., Johnson, K., Bradley, R., Grunwald, G. B., Cornel, E., Lilienbaum, A. and Holt, C. E. (1996). Cadherin function is required for axon outgrowth in retinal ganglion cells in vivo. *Neuron* **17**, 837-848.

Tepass, U., Truong, K., Godt, D., Ikura, M. and Peifer, M. (2000). Cadherins in embryonic and neural morphogenesis. *Nat. Rev. Mol. Cell Biol*. **1**, 91-100.

Thoreson, M. A., Anastasiadis, P. Z., Daniel, J. M., Ireton, R. C., Wheelock, M. J., Johnson, K. R., Hummingbird, D. K. and Reynolds, A. B. (2000). Selective uncoupling of p120ctn from E-cadherin disrupts strong adhesion. *J. Cell Biol.* **148**, 189-201.

Turner, D. L. and Weintraub, H. (1994). Expression of achaete-scute homolog 3 in *Xenopus* embryos converts ectodermal cells to a neural fate. *Genes Dev.* **8**, 1434-1447.

Uemura, K., Kitagawa, N., Kohno, R., Kuzuya, A., Kageyama, T., Chonabayashi, K., Shibasaki, H. and Shimohama, S. (2003). Presenilin 1 is involved in maturation and trafficking of N-cadherin to the plasma membrane. *J. Neurosci. Res.* **74**, 184-191.

Van Aelst, L. and Symons, M. (2002). Role of Rho family GTPases in epithelial morphogenesis. *Genes Dev.* **16**, 1032-1054.

Wacker, S., Grimm, K., Joos, T. and Winklbauer, R. (2000). Development and control of tissue separation at gastrulation in *Xenopus*. *Dev. Biol.* **224**, 428-439.

Xiao, K., Allison, D. F., Buckley, K. M., Kottke, M. D., Vincent, P. A., Faundez, V. and Kowalczyk, A. P. (2003). Cellular levels of p120 catenin function as a set point for cadherin expression levels in microvascular endothelial cells. *J. Cell Biol.* **163**, 535-545.

Yap, A. S. and Kovacs, E. M. (2003). Direct cadherin-activated cell signaling: a view from the plasma membrane. *J. Cell Biol.* **160**, 11-16.